Sm^{149} (n, α) REACTION CROSS-SECTION MEASUREMENT USING A GAS IONIZATION CHAMBER

By

CHARLES WAIN FRIEND

Bachelor of Science

Oklahoma State University

Stillwater, Oklahoma

1958

Submitted to the Faculty of the Graduate School of
the Oklahoma State University
in partial fulfillment of the requirements
for the degree of
MASTER OF SCIENCE
May, 1964

Sm^{149} (n, α) REACTION CROSS-SECTION MEASUREMENT

USING A GAS IONIZATION CHAMBER

Thesis Approved:

Thesis Adviser

Dean of the Graduate School

ACKNOWLEDGMENTS

The author wishes to express his appreciation and thanks to Dr. Matti J. Nurmia for his guidance and invaluable technical assistance on this project. Sincere thanks are due to Albert E. Wilson, Chief Reactor Operator, Oklahoma University, whose cooperation and interest greatly assisted in the experiments performed at the Oklahoma University Reactor Laboratory. The author also wishes to thank G. D. Loper for his assistance in the use of the analyzer and to thank and give credit to Heinz Hall and Richard Gruhlkey for construction of the ionization chamber and its components.

TABLE OF CONTENTS

LIST OF TABLES

LIST OF FIGURES

CHAPTER I

THEORY

A. Introduction.

The study of a particular (n, α) reaction belongs in the class of neutron interactions with nuclei. A general reaction equation for such interactions would be (3)

$$A + n \longrightarrow B + q + \ldots$$

A simple interaction can be written as A (n, q) B which states in compact notation that a neutron (n) interacts with a nucleus A to yield a nucleus B plus another particle q. In the case of elastic scattering A(n, n)A, the nucleus and incident neutron retain their same identities and total kinetic energy before and after interaction while in inelastic collisions A(n, n')A' the sum of the total kinetic energy changes. Other interactions between a nucleus and an incident neutron can include the radiative capture process in which the neutron is absorbed followed by emission of a gamma ray, a reaction between the target nucleus and incident neutron to yield a different nucleus and outgoing particle (as in (n, α) or (n, p) reactions), or fission processes in which an incident neutron is absorbed by the target nucleus which then splits into fission fragments. The conservation of total angular momentum, energy, and parity restricts the types of interactions possible for a given target nucleus and incident particle which makes it possible to predict or at least explain in most cases what occurs experimentally.

The cross section for an interaction is a measure of the probability that it will occur. The units of cross section are cm^2 or more commonly "barns" (10^{-24} cm^2). The cross section (σ) of a nucleus for an interaction is defined as (4, p. 2-6)

$$\sigma(cm^2) = \frac{\text{Number of interactions/sec}}{\text{Number of incident particles/sec-cm}^2} .$$

Thus for a particular source of area A (cm^2) containing N (nuclei/cm^3) having an incident flux of $F = \rho v$ where ρ is area density of particles (#/cm^2) and v is their velocity (cm/sec) we have:

$$\text{Total Interactions/sec} = A\ (cm^2)\ F\ \left(\frac{\#\ \text{Incident}}{\text{cm-sec}}\right)\ N\ \left(\frac{\#\ \text{Target}}{cm^3}\right)\ \sigma(cm^2).$$

Cross section can be physically interpreted as the perpendicular area that a nucleus presents to a flux of incident particles. This area varies depending on the type of nucleus and incident particle and on the total energy, angular momentum, and parity of the system.

"Total cross section" is a measure of the probability of all possible interactions occurring. With neutrons this is measured by sending a collimated beam of neutrons through a thin source, and from the transmission loss itself one can find the total cross section due to scattering, absorption, etc. Any particular reaction such as the Sm^{149} (n, α) reaction is studied as a "partial cross section", i.e., the probability of a particular reaction occurring in competition with other possible reactions.

B. Q Value calculations and decay scheme for Sm^{149}.

In order to examine the possibility of a reaction (partial) cross section for Sm^{149}, the following calculations are made for a (n, γ) reaction and a (n, α) reaction.

1. Calculation for the Sm^{149} (n, γ) reaction:

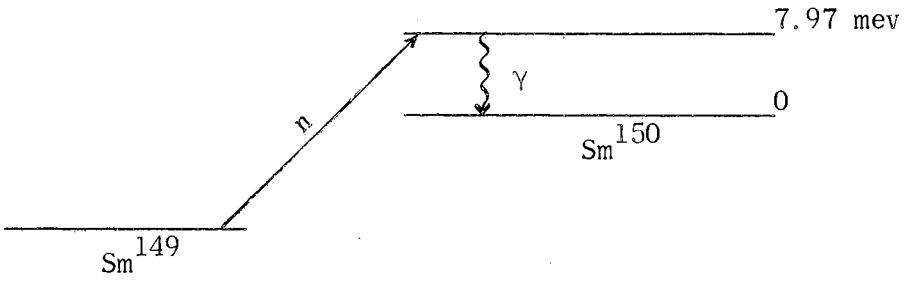

Figure 1. Sm^{149} (n, γ) Reaction Decay Scheme.

Mass data is from (5).

Sm^{149}	148.964	150	a.m.u.
+ n	1.008	982	
	149.973	132	
- Sm^{150}	149.964	570	
$(Sm^{149} + n) - Sm^{150}$ =	.008	562	a.m.u. x 931.1 mev/amu

Mass energy difference = 7.97 mev is the excitation energy available in Sm^{150} following absorption of a thermal neutron (disregarding negligible thermal energy of neutron). The gamma transition to ground level of Sm^{150} is the preferred mode of decay over 99% of the time.

2. Calculation of Sm^{149} (n, α) reaction:

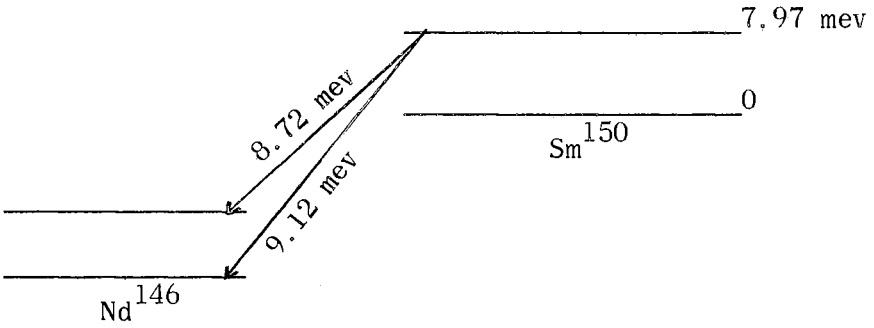

Figure 2. Sm^{149} (n, α) Reaction Decay Scheme.

MacFarlane and Almodovar (2) found two energies in the alpha spectrum of the Sm^{150} decay, a 9.12 mev alpha energy from Sm^{150} to ground level of Nd^{146} and a 8.72 mev alpha energy to a first excited level of 455 Kev

above ground level. The Q value calculation for this reaction is the following. Mass data is from (6).

Nd^{146}	145.959	08	a.m.u.
+ He^{4}	4.003	87	
	149.962	95	

from calculation on (n, γ) reaction

Sm^{149} + n =	149.973	13	
-(Nd^{146} + He^{4} -	149.962	95	
Mass difference	0.010	18	a.m.u.

x 931.1 mev/a.m.u.

Mass energy difference = 9.48 mev.

Hence the Q value gives the energy available to be shared by the recoiling nucleus and alpha particle following disintegration. Using the letter N for nucleus and α for alpha particle, the maximum kinetic energies are

$$T_N = \frac{M_\alpha}{M_\alpha + M_N} Q \qquad T = \frac{M_N}{M_\alpha + M_N} Q.$$

This means that potentially an alpha particle has a kinetic energy of a little above 9 mev over the attractive potential well of the Nd^{146} nucleus. This is still less than the coulomb barrier of the nucleus, but there is a finite probability that it can get out. This probability can be expressed in terms of a decay constant λ for which a calculation can be made using the Bethe equation (7, p. 8) or it can be calculated more easily in terms of the half life $T_{1/2}$ using an approximation to the Bethe equation by M. Nurmia and R. Taagepera (7, p. 10). The high neutron absorption cross section of Sm^{149} of 39,900 barns (8, p. 50) makes this alpha decay experimentally possible to observe.

C. Thermal Neutron Flux Considerations.

The source of neutrons in this experiment was a thermal column in the Oklahoma University swimming pool type reactor (Aerojet AGN 211). The neutrons came from a controlled chain reaction taking place inside the core of the reactor. By repeated collisions within the moderator surrounding the reactor core, the neutrons came close to thermal equilibrium with the moderator. The velocity distribution of these neutrons exhibited the Maxwell distribution: (4, p. 152)

$$N(v)\,dv = \frac{4\,N_t}{v_o^3\,\sqrt{\pi}}\,v^2\,e^{(v/v_o)^2}\,dv,$$

where v is the velocity of the neutrons, N(v) is the density of neutrons per unit volume as a function of velocity, N_t is the total number per unit volume, and v_o is the most probable velocity at the moderator temperature. This most probable velocity at 293.7^{o}K is 2200 m/sec for a thermal neutron energy of 0.0253 ev which is the standard neutron velocity quoted in most literature of today. It is of interest to note that the de Broglie wavelength of a neutron at this velocity is 1.8 Angstroms which is the order of soft x-rays. Hence in "neutron optics" the scattering phenomena of thermal neutrons is analogous to x-ray scattering of similar wavelength, and velocity selection of the neutrons can be accomplished by crystal (like beryllium) diffraction of a neutron beam. This is used to get specific neutron energies for cross section measurements such as determining the "f factor" of a source to be discussed later in this same section.

The neutron distribution at Oklahoma University is said to be a hardened distribution in that the water moderator surrounding a graphite

jacket which partially shields the core is kept at a temperature of 25^{0} C while the average temperature of the thermal neutron flux is 55^{0} C. (9). This means the actual flux will have a larger fast to thermal ratio than it would have if it were actually at the temperature of the moderator. The fast neutrons are the portion of the flux which will give a background pulse spectrum in a gas ionization chamber, as explained in Chapter III, Part C of this thesis.

The thermal neutron temperature of the neutron flux used in making a cross section measurement is thus an important part of the data, particularly for a measurement on an isotope like Sm^{149} which has a neutron absorption resonances in the thermal region its average absorption cross section for a Maxwellian distribution follows a $\frac{1}{v}$ (where v is neutron velocity) relationship, i.e., $\sigma_a = \frac{\text{constant}}{v}$. (4, p. 157, also derivation p. 24-27). For such materials, a cross section measurement made at a neutron flux temperature slightly higher than 293^{0} K will be the same as one made at 293^{0} K within negligible error. However, when a neutron resonance occurs in the thermal neutron region as it does for Sm^{149} at .0967 ev. (8, p. 47), it is necessary to use a correction factor "f" (4, p. 160) which gives the deviation of the material from a $\frac{1}{v}$ cross section standard of the 2200 m/sec neutron flux by dividing the effective cross section found experimentally σ (n, α) by the f factor for that neutron flux temperature to get σ_0 (n, α). This is demonstrated in the results of MacFarlane and Almodovar, (2) Table II. The f factor for a neutron flux temperature of 55^{0} C (328^{0} K) was found using the results of Pattenden (8, p. 51) which gives f values of

$$f\ (300^{0}\ K) = 1.720; \quad f\ (350^{0}\ K) = 1.922.$$

Since it is correct to take the interpolation as approximately linear, then f (328^{0} K) = 1.83.

D. Comparative Method of Obtaining Cross Section Values.

The basic concept in this technique is to use a mixed source which contains a known amount of an isotope which has a reaction in a neutron flux that can be compared to the source reaction of the Sm^{149} (n, α). This eliminates the need to know the actual value of the neutron flux or counter geometry.

Using a source of mixed natural samarium and chemically separated uranium, the first step in this method is to make a determination of the amount of Sm^{149} and U^{235} present by determining over a timed interval the number of U^{238} alpha counts and the number of Sm^{147} alpha counts and then use decay constants and natural isotopic abundance ratios for each. (See Table I.) Next by inserting the source into the neutron flux of a reactor, and using the fission cross section of U^{235}, the number of fission fragments counted can be related to the flux. Then by counting the (n, α) reaction alphas of Sm^{149} and using the flux relationships from the U^{235} fissions, the Sm^{149} (n, α) cross section can be determined.

TABLE I

URANIUM ISOTOPE DATA

Isotope	Abundance %	Half Life (years)	Prominent Alpha Energies (mev)
U^{234}	.0056	2.48×10^{5}	4.72 ; 4.77
U^{235}	0.721	7.13×10^{8}	4.40 ; 4.58
U^{238}	99.27	4.51×10^{9}	4.18

Data is from (10).

Actually it is the counts ratios that are important as will be shown in the following derivation of the cross section formula for this experiment:

1. Amount of U^{235} in source.

The total alpha activity of the uranium source will be the sum of the partial activities of each isotope,

$$A_t = A_{234} + A_{235} + A_{238}.$$

Activity is defined in terms of the decay constant λ and the number of atoms present, N, e.g., $A_{238} = \lambda_{238} N_{238}$. The isotope U^{238} decays by alpha emission with a half life $T_{238} = 4.51 \times 10^9$ yrs as the parent of a radioactive chain with U^{234} as an alpha active daughter having a half life of $T_{234} = 2.48 \times 10^5$ yrs. It follows that the alpha activities of U^{238} and U^{234} will be in secular equilibrium since the daughter is much shorter-lived than parent (11). This means

$$\lambda_{238} N_{238} = \lambda_{234} N_{234}.$$

The U^{235} present makes a contribution to the total alpha particle activity in the energy range between the alphas of U^{238} and U^{234}. The ratio of activity of U^{235} to U^{238} is

$$\frac{A_{235}}{A_{238}} = \frac{0.721\%}{99.27\%} \frac{4.51 \times 10^9 \text{ yrs}}{7.13 \times 10^8 \text{ yrs}} = 0.046.$$

Therefore if one counts the total alpha activity of a uranium source between 4.18 mev and 4.77 mev, the total activity is

$$A_t = A_{234} + A_{235} + A_{238} = 2.046\, A_{238}.$$

and

$$N_{238} = \frac{A_t}{(2.046)\ \lambda_{238}} = \frac{A_t T_{238}}{(2.046)\ 0.693}.$$

Half life is defined as $T = 0.693/\lambda$. Then by isotopic abundance the number of N_{235} atoms will be $N_{235} = \frac{0.721}{99.27} N_{238}$.

2. Amount of Sm^{149} in source:

Activity of $Sm^{147} = A_{147} = \frac{.693}{T_{147}} N_{147}$.

Isotopic Abundance of Sm^{147} is 14.97% and of Sm^{149} is 13.83%. (12)

Therefore

$$N_{149} = \frac{13.83}{14.97} \frac{T_{147}}{.693} A_{147}.$$

3. Taking into account the almost negligible Sm^{147} (n, α) reaction. The results of the Israel AEC research group (1) show that there is approximately a 1.8% additional alpha contribution due to the Sm^{147} (n, α) reaction to the total alpha activity observed in the experimental range of interest during neutron irradiation. Therefore the total (n, α) activity is

$$A(n, \alpha) = 1.018\ A_{149}(n, \alpha).$$

4. Flux measurement using U^{235} fission fragments. There are two fission fragments and hence two counts per each fission. Letting the symbol A_f represent the number of fission fragment counts, one finds

$$\#\text{ of fissions} = 1/2\ A_f$$

and

$$\#\text{ of fissions} = (\text{Flux})\ \sigma_{235}N_{235} = 1/2\ A_f$$

Therefore

$$(\text{Flux}) = \frac{A_f}{2\ \sigma_{235}N_{235}}.$$

5. σ(n, α), the effective cross section for Sm^{149} (n, α).

The Sm^{149} (n, α) alpha activity = A_{149} = (Flux) σ(n, α)N_{149}. Solving for σ and using results from part 3 for A(n, α) and part 4 for (Flux), one finds

$$\sigma(n, \alpha) = \frac{A(n, \alpha)}{1.018} \frac{2\sigma_{235}}{A_f} \frac{N_{235}}{N_{149}}.$$

Using results from parts 1 and 2 of this section, the formula becomes

$$\sigma(n, \alpha) = 2\sigma_{235} \frac{.714}{99.28} \frac{A_t}{2.046} \frac{T_{238}}{.693} \frac{14.97}{13.83} \frac{.693}{T_{147}A_{147}} \frac{A(n, \alpha)}{(1.018)A_f}.$$

Substituting in values from part 1 and (10) where

$$T_{147} = 1.06 \times 10^{11} \text{ yrs.} \quad \text{and } \sigma_{235} = 580 \text{ barns,}$$

the resulting equation for effective cross section is

$$\sigma(n, \alpha) = 186_{\text{millibarns}} \frac{A_t}{A_{147}} \frac{A(n, \alpha)}{A_f}.$$

CHAPTER II

EXPERIMENTAL PROCEDURE, APPARATUS, AND SOURCE PREPARATION

A. General Concept of the Experiment.

In order to induce the Sm^{149} (n, α) reaction it is necessary to introduce a source containing that isotope into a thermal neutron flux of a reactor. The source for this experiment was natural samarium containing the Sm^{149} isotope which was plated in vacuum on an aluminum source plate. The source plate was painted with a dilute uranyl nitrate solution, dried, and formed into a cylinder for insertion into the ionization chamber. The Oklahoma University swimming pool type nuclear reactor (Aerojet AGN 211) used in this experiment had a four-inch diameter horizontal thermal neutron port tube which extended through the water and just up to the graphite jacket of the core. The ionization chamber and the electronic preamplifier connected to the chamber formed a three and one-half inch diameter cylindrical unit which permitted easy insertion into the thermal neutron port.

The ionization pulses coming from the chamber were amplified by the preamplifier connected directly to the chamber and were then transmitted through cables out of the reactor and into a 512 channel pulse height analyzer. This analyzer (Nuclear Data - ND 130) stored the pulses depending on their voltage height which varied linearly with the alpha particle energy creating the pulse. The stored data from the analyzer

were typed out using special circuits of the analyzer which were coupled to an IBM electric typewriter. (See Figure 3.)

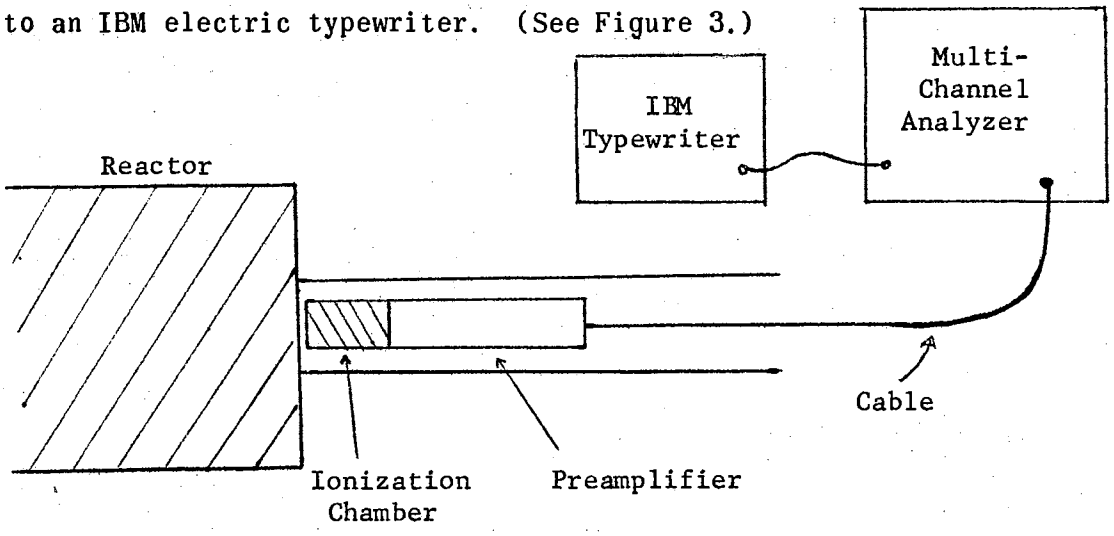

Figure 3. Block Diagram of Basic Components in Experimental Setup.

In the experiments described in this thesis, the reactor runs were about 10 minutes duration at an approximate power level of 1 watt for about 3 minutes of live analyzer time, i.e., the actual pulses coming from the ionization chamber have turned the analyzer on for successive periods totaling 3 minutes. This proved to provide a good balance between the Sm^{149} alpha peaks, the fission fragment counts, and the background in the ionization chamber due to the collisions of fast neutrons with the methane molecules in the gas mixture (90% Argon-10% Methane) which caused ionization pulses due to proton recoil. (See example spectrum, Figure 4.) The total counts per channel were typed out and then plotted on graphs by hand. The background due to the proton recoil and any due to the fission fragment tail extending under the (n, α) peak was subtracted out, and the resulting counts of Sm^{149} alphas and the fission fragments were totaled. (See Chapter III, Part A.) The ratio of the total counts of Sm^{149} alphas to number of fission fragments (2 per fission) was used in the calculations pertaining to cross section. (Also see Chapter I,

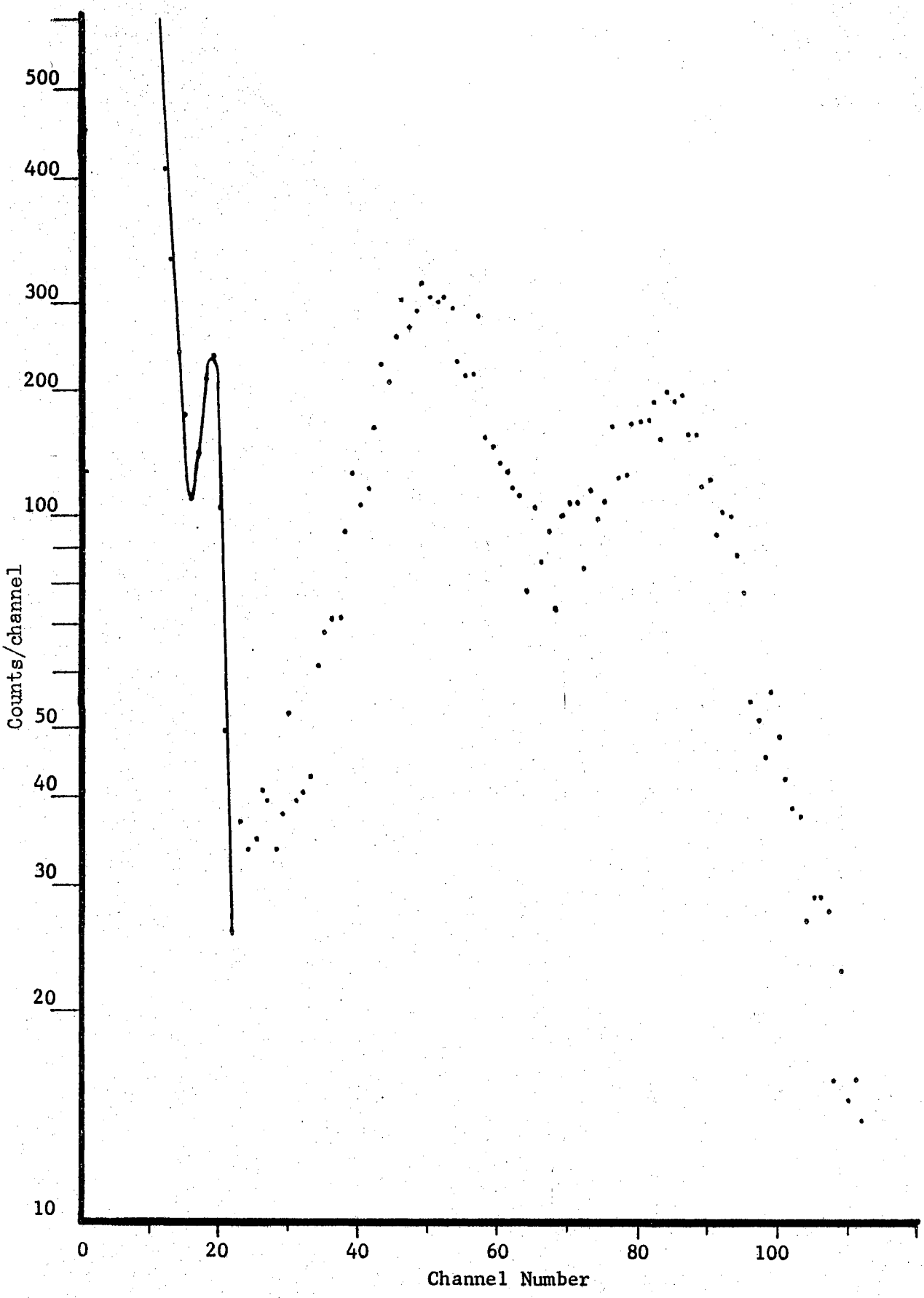

Figure 4. Sample (n, α) and Fission Fragment Spectrum (Source #1, Run #4)

Part D.) The calibration of sources to determine the ratio of the quantity of Sm^{149} to U^{235} was done by making experimental runs outside the reactor using the same ionization chamber.

B. Description of Ionization Chamber.

The ionization chamber is a device which collects the electrons formed by a primary ionizing particle, such as an alpha particle, as it passes through a gas. An alpha particle will lose approximately the same increment of energy per ion pair formation (approximately 30 ev per ion pair in most nuclear counter gas mixtures). The electric field imposed on the system should be sufficient to keep ion pairs separated after the ionizing particle passes through the gas and to move the electrons and positive ions formed to the respective electrodes. However, the field should not be so intense as to cause acceleration of ions and electrons thus creating secondary ionization (13). The ionization chamber used in this experiment was a cylindrical gridded type chamber. The cylindrical design was chosen to present as large a source area as possible to the neutron flux of the reactor. (The source was plated on an aluminum sheet which was then shaped into a cylinder and inserted into the chamber touching the inner wall.) The electric field at some radial distance R between the center collector electrode of radius R_c and the interior surface of the grounded cylinder wall (source plate) of radius R_a is

$$E_{(R)} = \frac{V}{R \ln \frac{R_c}{R_a}},$$

where V is the potential between the two electrodes. (14, p. 20).

This relationship shows that the electric field is most intense near the inner electrode. This characteristic has a definite effect on where one can interpose a grid between the collector rod and source wall to get maximum resolution. A grid is used to initially shield the collector from the change in electric field when an alpha particle passes through the gas forming positive ion and negative electron pairs. The grid voltage is some intermediate value between the high voltage (positive) collector and the grounded source wall. The screen grid is made of a thin widely separated wire mesh which allows it to electrostatically shield but prevents it from capturing any sizeable number of the electrons formed by the ionizing particle. However, when the electrons formed pass through the grid, the effect of the field due to their motion immediately takes effect inducing charge on the collector. Without a grid, the effect of the change in the electric field due to the electrons is to induce a change of the total charge on the center collector rod as soon as the ionizing particle starts through the gas. (See Figure 5, Part A.) This makes a longer output pulse with a slower rising slope and rounded-off peak as seen when electronically amplified and viewed on an Oscilloscope. (See Figure 5, Part B.)

The effect of the grid is to electrostatically shield the collector while the ionizing particle is forming ion pairs between the source plate and the grid. (See Figure 5, Part C.) Then as the positive ions and negative electrons separate, the collector senses the change in electric field as the electron cloud moves through the grid. This produces an output pulse which has a steep initial slope and well defined peak. (See Figure 5, Part D.) This makes pulse height analysis of the

grid:

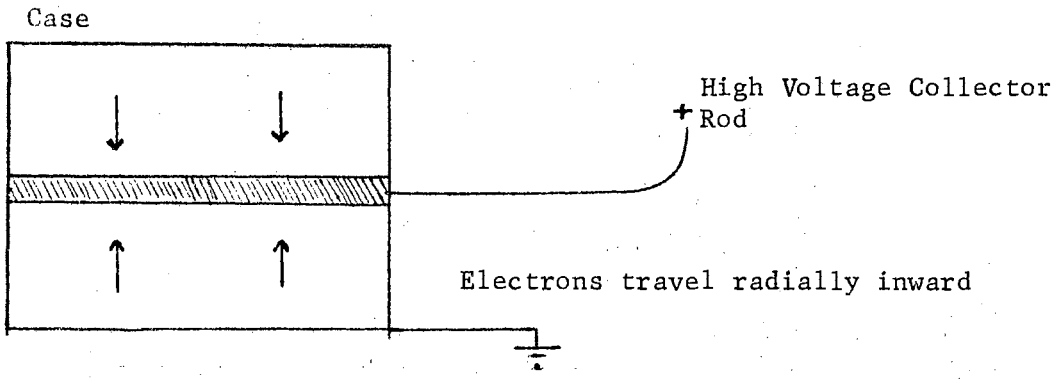

Part A. Ionization Chamber Without Grid.

Part B. Output Pulse of Ionization Chamber Without Grid.

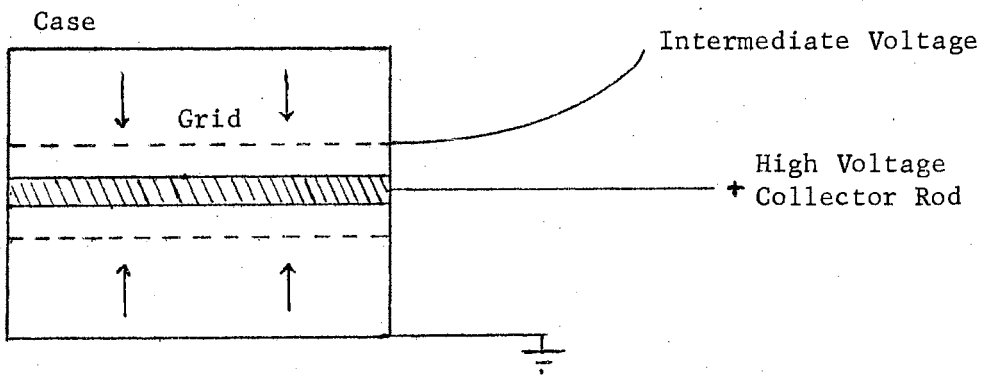

Part C. Ionization Chamber with Grid.

Part D. Output Pulse of Ionization Chamber with Grid.

Figure 5. Cylindrical Ionization Chamber Basic Diagrams.

incoming pulse more accurate and decreases the time between pulses which can be separately analyzed. (To be accepted by an analyzer, the pulses' initial slope and peaks must be separately distinct.) Thus faster counting rates for a chamber are possible.

The actual chamber (see Figure 6) was constructed from a 3.50 inch solid cylinder of aluminum and bored out to a 3.00 inch inside diameter leaving one end closed. The open end was threaded to accept an aluminum base plate. The collector rod extends into the chamber as shown through a teflon (plastic) sleeve which insulates it from the grounded outer case. The grid is mounted on aluminum notched disks which fit around the collector rod and are insulated from it and the case by the teflon sleeves. The grid voltage is supplied by a separate lead entering the chamber through a separate port and insulated by a teflon sleeve.

A serious difficulty was sealing the ionization chamber at the sleeve inserts. The solution found was to use epoxy cement (a particular plastic resin cement) which would adhere both to aluminum and teflon. All the components were cemented together at the two inserts.

The aluminum material for the chamber had been chosen to eliminate any material having an (n, α) reaction besides the source material. However aluminum (Al^{28}) has a short lived Beta activity induced by neutron absorption by Al^{27}. The Beta activity of the ionization chamber, amplifier chassis, and aluminum housing caused the experimenters to not be able to handle the unit after it was pulled from the reactor for 2 to 3 minutes. This slowed down the changing of sources in the chamber. The Beta particles had no serious effect on the measurements made as proven by using the chamber in the reactor without a source. The activity would not affect most (n, α) or (n, p) measurements. Nevertheless, it might

be better to make the chamber and its components out of mild steel material containing no reactive elements in order to avoid residual activity. One final improvement made was to mill down the outside diameter of the chamber to 3.25 inches leaving the base plate at 3.50 inches. This reduced as much as possible any aluminum shielding of neutron flux and cut down induced residual radioactivity which was of course strongest in that part of the unit closest to reactor. There was a slight problem in having aluminum screw threads on the base plate screwing into an aluminum case because they naturally tend to bind and strip. The approach to use would be to cut large threads and keep them lubricated. The O ring sealing of the gas chamber where the base plate screwed into the chamber case proved quite adequate to hold any gas pressure desired for experiments.

The resolution of this chamber was amazingly good. It was used for measuring other known alpha activities in the laboratory and produced as clearly defined spectra as did the parallel plate gridded ionization chambers used previously and described by Sievers (15).

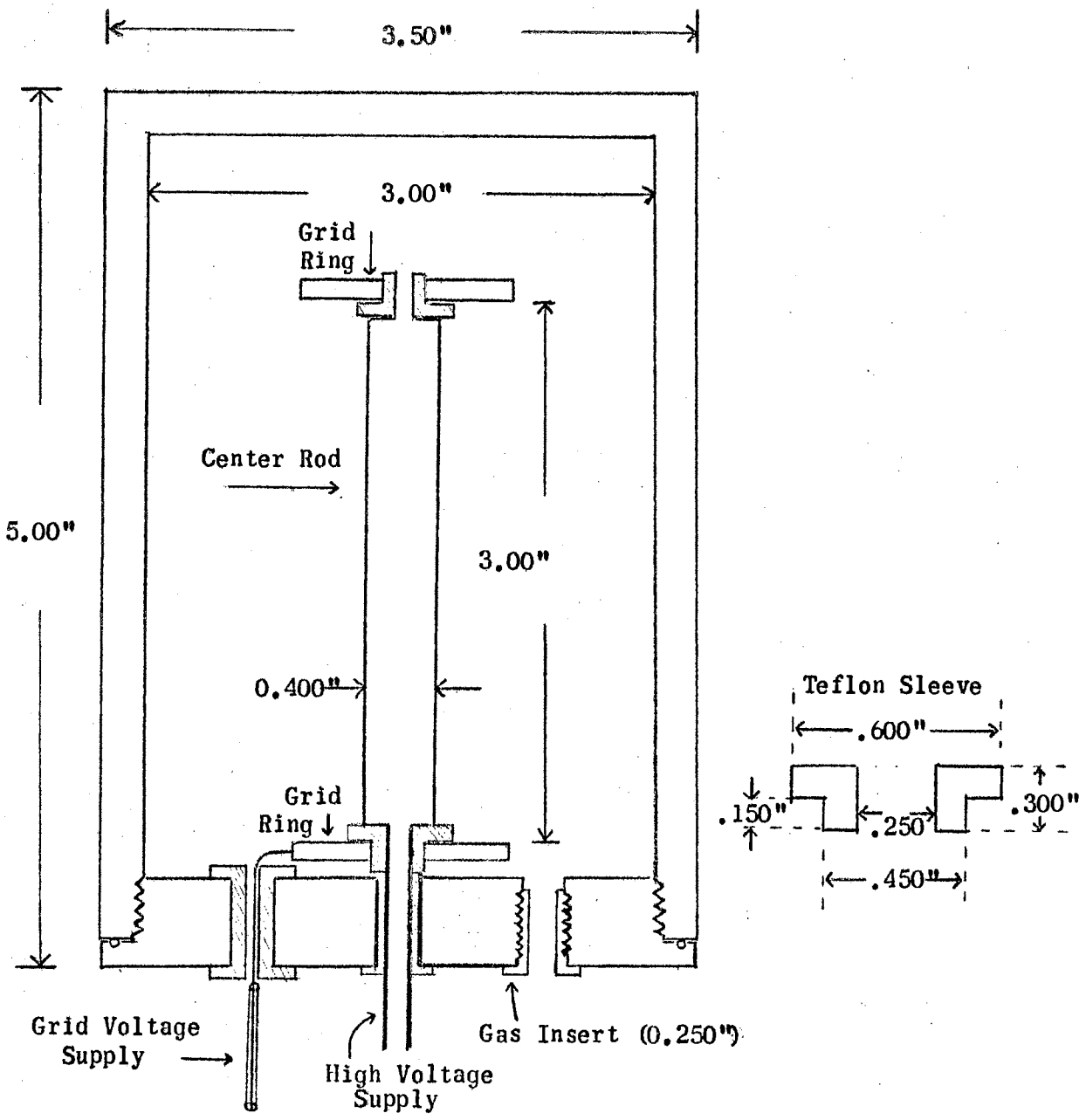

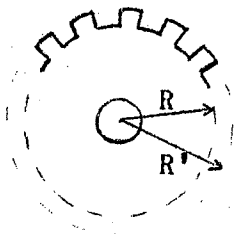

R = 0.500"

R'= 0.600"

Grid Ring
(Center hole diameter of bottom one in sketch is 0.250", top one is 0.450")

All parts are aluminum material except for Teflon sleeves in Base Plate and a steel nut used on end of Center Rod outside of chamber.

FIGURE 6. Construction Diagram of Ionization Chamber.

C. Description of Electronic Preamplifier.

It is necessary to have a preamplifier connected directly to an ionization chamber in order to receive and amplify the ionization pulses coming from the chamber for transmission through cables to a pulse height analyzer outside the reactor. If the cables were connected directly to the ionization chamber and pulses transmitted to an amplifier outside the reactor, the attenuation would drastically affect the resolution of the pulses. Hence a preamplifier was designed to fit into a cylindrical case directly behind and attached to the ionization chamber. The electronic circuits of this cascode feedback amplifier were designed by Dr. Matti Nurmia. Schematic layout of preamplifier circuits is shown in Figure 8, Part A. The actual design uses three (3) double triodes (tube type 6922) in four stages. (See Figure 9.)

The first stage of the preamplifier (Figure 9, Tube A) is the cascode amplifier stage (16). A simplified diagram of this stage is shown in Figure 8, Part B. This circuit behaves like a pentode having an amplification $A \approx - gmR$, but has the low noise advantages of the triode with no screen current needed. This circuit is widely used in nuclear physics instrumentation particularly as a first stage in preamplifiers because of its low noise and high gain characteristics.

The next stage is a single stage triode amplifier (Figure 9, Tube B-1) which is coupled directly to an inverse feedback circuit (Figure 9, Tube B-2). The inverse feedback circuit is widely used in nuclear physics instrumentation to provide negative feedback that will counter variations in power supply voltage (plate supply) and changes in the circuit component characteristics and to improve linearity of

the amplifier. The fraction of output voltage (β) which is fed back is easily seen from the schematic diagram of a simple cascaded triode amplifier. (See Figure 8, Part C.) The value of β comes from the voltage divider relation $\frac{R_2}{R_1 + R_2} = \beta$. It can be shown (14, p. 81) that if the over-all gain G of the first two stages is large and $G\beta$ is large, then the amplification of this amplifier $A = 1/\beta$. Hence in the preamplifier built for this experiment one expects

$$A = \frac{R_1 + R_2}{R_2} = \frac{33K + .3K}{.3K} = 110 ,$$

since the last stage of this preamplifier is a cathode follower circuit which does not basically change the gain.

The last stage (Figure 9, Tube C-1), a cathode follower circuit, characteristically has high input impedance and low output impedance. This means it will not draw any appreciable current from the amplifier stages behind it, and it can be used to couple the preamplifier to a low impedance load.

Heater noise (a.c. ripple from 6.3 a.c. supply to heaters of tubes) was reduced by connecting the heater leads coming into the amplifier across a potentiometer. (See Figure 7.) The grounded center tap of the potentiometer is varied until any a.c. hum in the output signal of the preamplifier is canceled out. This device is called a hum balance.

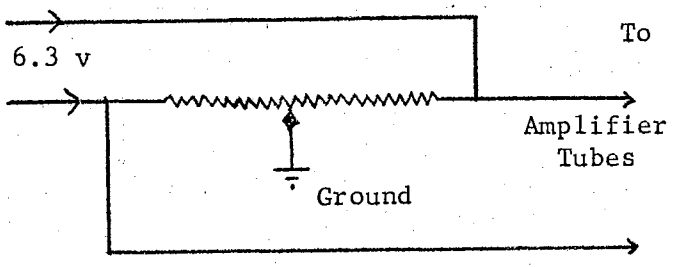

Figure 7. Hum Balance Diagram.

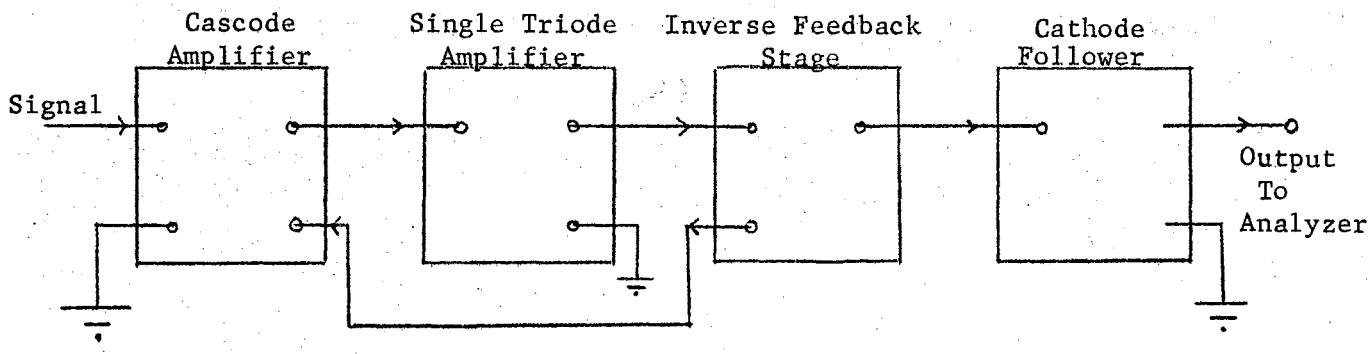

Part A. Block Diagram of Preamplifier Components.

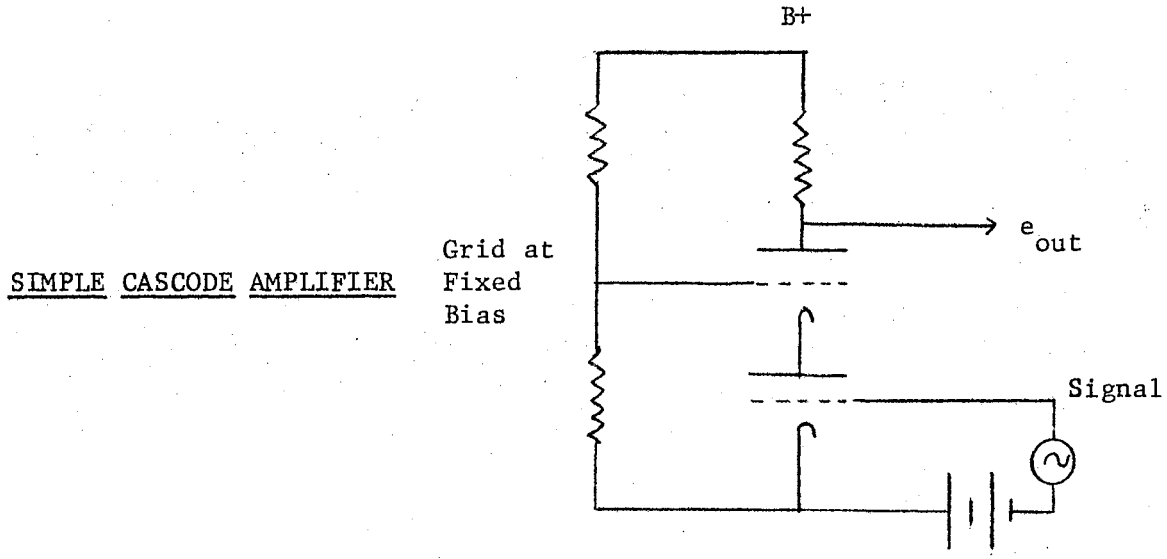

Part B. Basic Cascode Amplifier.

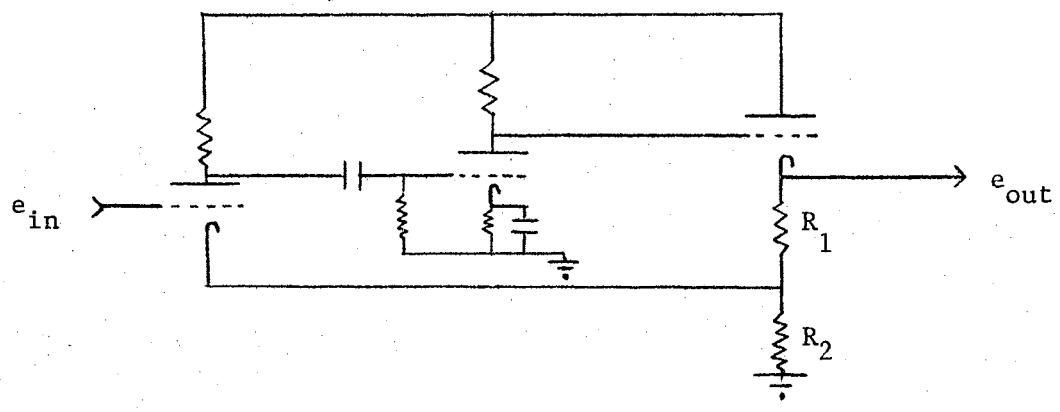

Part C. Basic Cascoded Triode Amplifier with Inverse Feedback.

Figure 8. Electronic Preamplifier Basic Diagrams.

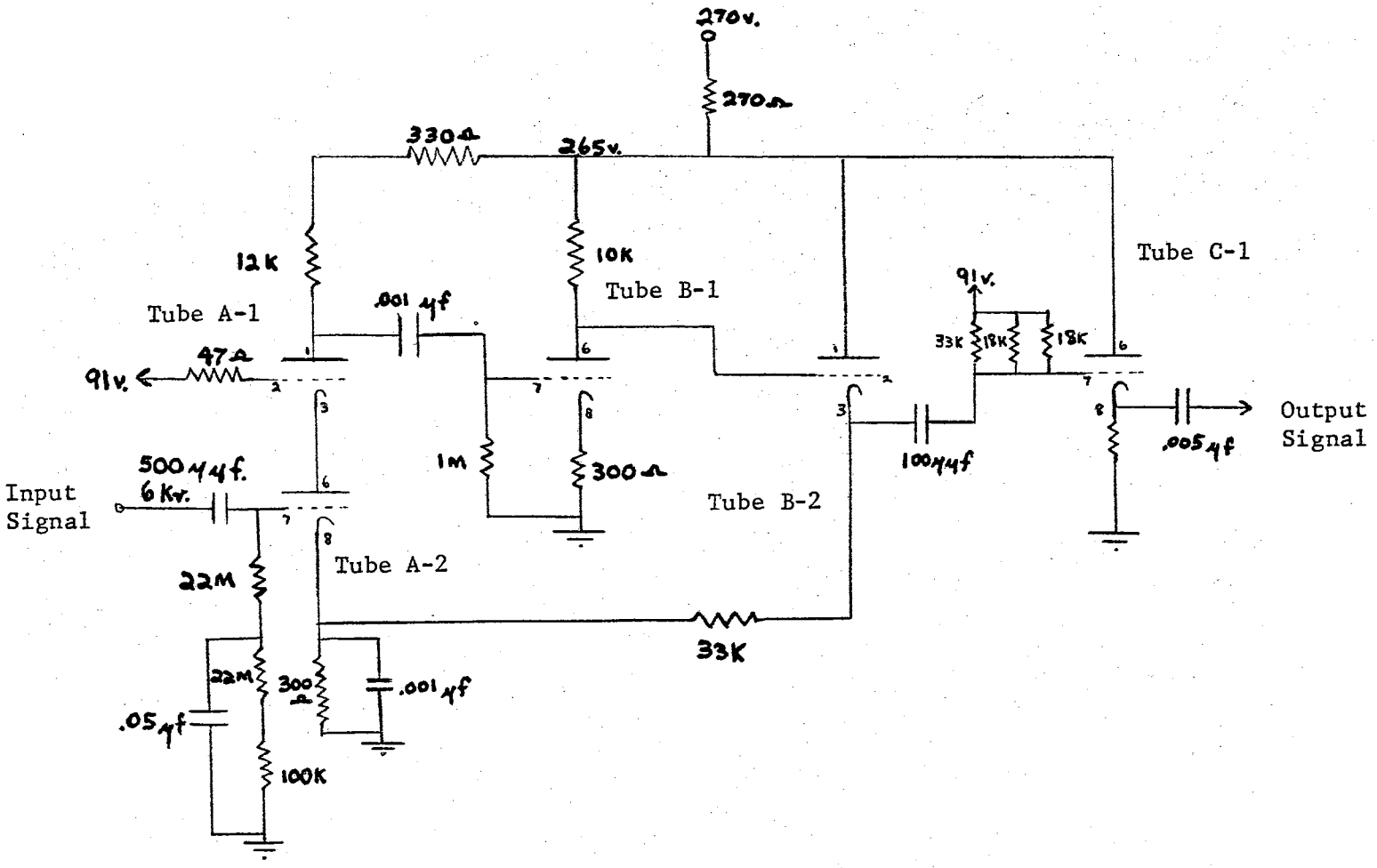

Figure 9. Electronic Preamplifier Circuit.

D. Ionization Chamber Center Rod and Grid Potential Circuit.

The center rod of the ionization chamber should be held at some static potential value between 1000 to 1200 volts. This is accomplished by connecting a high voltage supply to the center rod through an RC network as shown in Figure 10 to minimize effect of random fluctuations or a.c. ripple from the high voltage supply. The cylindrical grid surrounding the center rod must be kept at some potential intermediate between the high voltage of rod and ground potential of the walls of the chamber. A simple voltage divider made of a series of resistors with an R.C. filter supplies this potential. The circuit at the bottom of Figure 10 is the plate supply for preamplifier showing a voltage divider constructed of resistors across a 10-10-10-μf (electrolytic can capacitor). The grid voltage bias of 91 volts for the cascode amplifier is a part of this circuit.

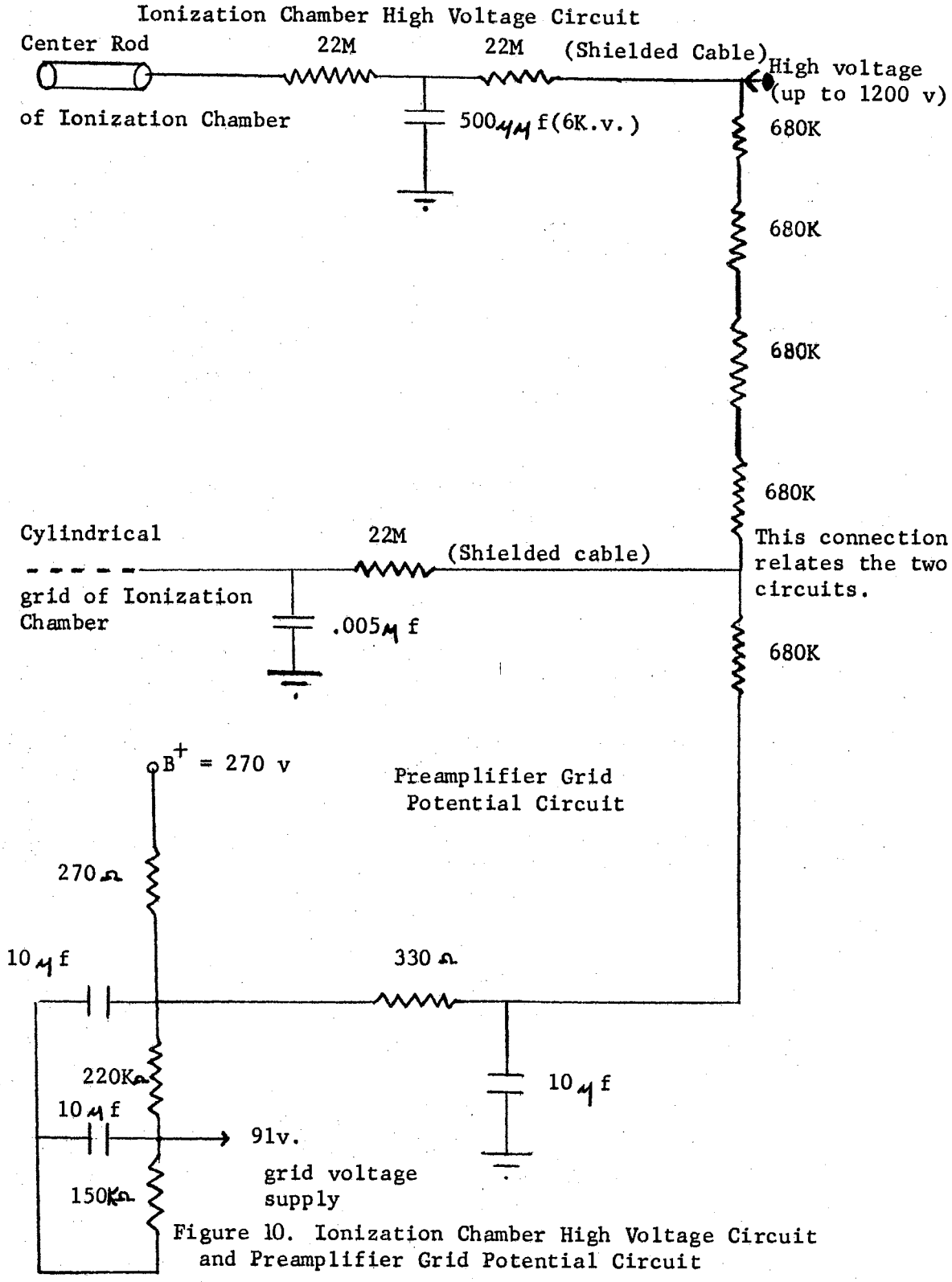

Figure 10. Ionization Chamber High Voltage Circuit and Preamplifier Grid Potential Circuit

E. Preamplifier Chassis, Holding Bracket, and Case.

The actual preamplifier was built on an aluminum chassis as shown in Figure 11, Part A. The three triode tubes with bases and the 10-10-10 μf electrolytic can type capacitor were placed in a downward position along the center of the chassis. Position of potentiometer is shown. The bracket to which this chassis was attached is shown in Figure 11, Part B. The bracket with preamplifier chassis mounted on top was attached by the bracket flanges to the top cover of the ionization chamber. The electronic tubes and can capacitor were positioned to hang straight down inside the bracket so the entire unit could remain in a 2 1/4" x 2 1/4" x 9" package which could be easily housed inside a 3 1/2" diameter aluminum cylinder. An aluminum cylinder was cut from thin aluminum tubing and was used to encase the preamplifier. (See Figure 11, Part C.) A bracket was built at one end to support the 1/4" diameter aluminum gas tubing which extended the length of the cylinder and into the ionization chamber. The 3 1/2" diameter case was attached to the ionization chamber which was also 3 1/2" in diameter by milling down the top cover plate until the cylindrical case could slip over it to a depth of 1/2". Screws were used to hold the case in place.

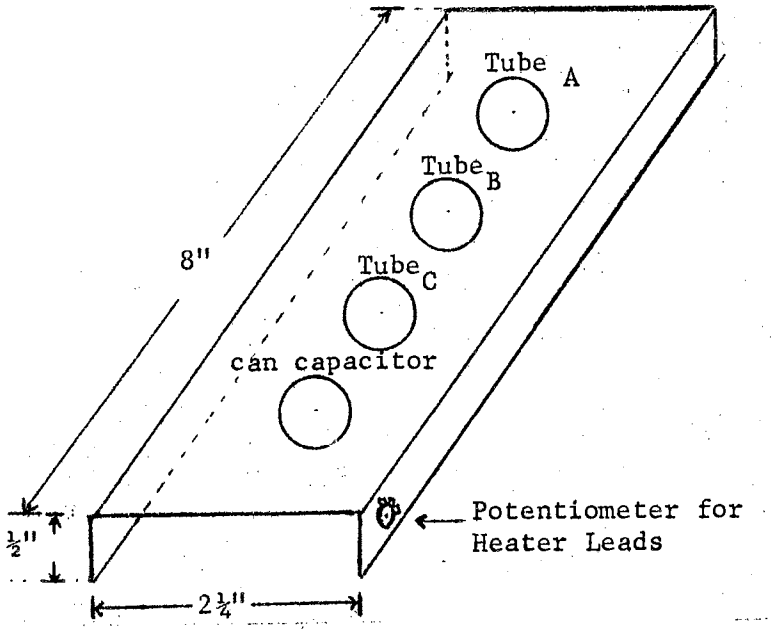

Part A. Preamplifier Chassis.

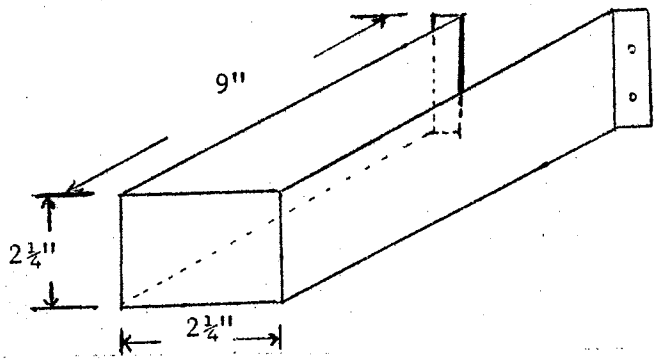

Part B. Preamplifier Holding Bracket.

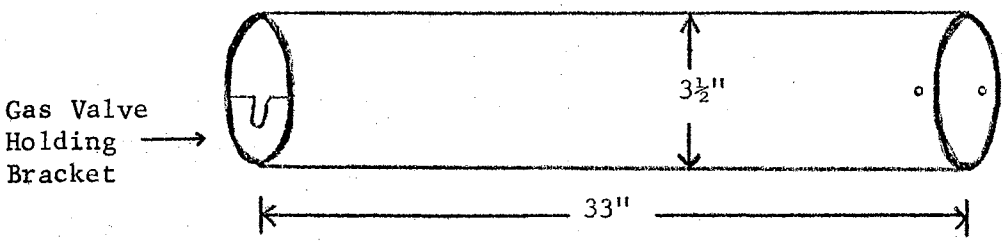

Part C. Preamplifier Case.

Figure 11. Preamplifier Chassis, Holding Bracket, and Case Construction Diagrams.

F. Gas System.

A gas system had to be designed in order to fill and flush the ionization chamber with a nuclear counter gas mixture (90% Argon-10% Methane). (See Figure 12.) "Swage lok" fittings were used for the insert into the chamber, gas valves, and T joints to hold the 1/4" diameter aluminum tubing. These fittings grip the tubing by ferrules tightening around the tubing when pressure is applied on them by a cammed-inner-surface nut. The gas enters the chamber through the T joint with valve #2 open and valve #1 closed. Then the gas coming into the T joint is cut off and valve #1 is opened to allow gas from the ionization chamber to be exhausted. This process repeated several times flushes the chamber clearing out air that is present due to insertion of the source. All joints should be gas tight. It is particularly essential that the joints from valve #2 on into the chamber be gas tight to maintain a specific gas pressure during a reactor run. It was found necessary to seal the gas insert into the chamber using epoxy cement, but with more careful machining this might not be necessary. The above arrangement also had the advantage that the gas pressure during the reactor run can be changed without removing the ionization chamber and preamplifier unit from its position by simply connecting a gas hose to the T joint and leaving valve #1 closed and valve #2 open. Then different spectra from the same source, neutron flux, and position may be taken at different gas pressure until the best resolved spectrum appears. The aluminum gas tubing which extended the entire length of the cylindrical case had to pass through the length of the preamplifier bracket and into the ionization chamber. Holes for

the gas tubing had to be bored in the bracket, and the position of the tubing had to be considered when laying out the electronic circuits on the preamplifier chassis as well as drilling the gas insert hole into the ionization chamber base plate.

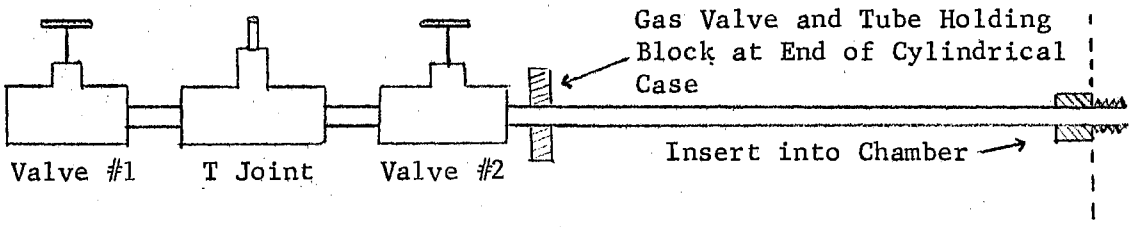

Figure 12. Basic Gas System Diagram.

G. Source Preparation.

In order to make a measurement of the cross section of the Sm^{149} (n, α) reaction, it was necessary to know the exact amount of samarium present in the source, the exact neutron flux incident on the source, and the counter geometry or to have a relative comparison between the Sm^{149} (n, α) reaction and a known reaction taking place in the same neutron flux. As indicated previously, the latter technique was the one used in this experiment.

Since the interior dimensions of the ionization chamber were 3.00 inches diameter and 4 3/8" in height, the source plates were cut from thin aluminum sheets in dimensions of about 9.4" x 4.25" in order to form a cylinder inside the chamber and be in contact all the way around with the cylindrical wall surface.

The samarium part of the sources was vacuum plated in the following manner. The samarium metal was cut from a small block into pieces about the size of buckshot. These pieces were placed into formed tantalum boats (a strip of tantalum crimped into a shallow V-shaped receptacle which can hold molten metal and has tabs for electrical contact). The boats were clamped inside a vacuum bell jar between two electrical conducting bars. The aluminum source plate was clamped above the boat; the best position for uniform plating being determined by experience. After the bell jar had been evacuated down to about 10^{-5} mm Hg of pressure, the tantalum boats were heated to a dull red color by allowing current to pass through them. The samarium metal melted into a globule, evaporated, and then plated out on the source plate above the boat. Care had to be exercised to not heat the samarium metal too rapidly or it would jump out of the

boat receptacle and also plating would not be as uniform. The idea was to plate the source plate with sufficient samarium yet thin enough not to appreciably attenuate alpha particles formed in the source.

The uranium was deposited in a very thin layer over the samarium by painting the source plate with a dilute solution of uranyl nitrate and then drying the source using heat.

CHAPTER III

CALCULATIONS AND RESULTS

A. Data Analysis Method.

The data in this experiment were typed out by an IBM electric typewriter in counts per channel from the 512 channel analyzer. Actually only 127 channels were used for convenience, and a typical data sheet is shown in Figure 13. Run #6 from Source #1 will be used as an example for the data analysis method:

1. The data from Run #6 for channels 8 through 35 were plotted on semilog paper using the linear scale for channel number and the logarithmic scale for counts/channel. (See Figure 14.)

2. The exponential tail of the proton recoil spectrum due to the fast neutron distribution passing through the gas counter mixture exhibits a straight line slope on a semilog plot. This slope can be linearly extrapolated through the (n, α) peak enabling one to subtract out the proton recoil contribution to the alpha peak.

3. The exponential tail of the fission fragment spectrum also exhibits a straight line slope on a semilog plot. Using a linear extrapolation of the slope of this line one can subtract out the fission fragment contribution to the alpha peak.

4. The resultant (n, α) peak can be plotted on linear paper with the fission fragment spectra (see Figure 15) or, with experience, one can simply list the resultant counts/channel over the (n, α) peak

in a tabular form taking the counts/channel over the fission fragment spectra as unchanged in general from the original data sheet. (See Table II.)

TABLE II

CALCULATED COUNTS PER CHANNEL FOR (n, α) PEAK
(SOURCE #1, RUN #6)

Channels	13	14	15	16	17	18	19
(From Original Data) Counts/channel	332	231	251	304	299	184	71
From Graph (p. 32) Proton Recoil Background	-215	-110	- 57	- 30	- 16	- 9	- 5
Sub total	117	121	194	274	273	175	66
From Graph (p. 32) Fission Fragment Tail	- 21	- 23	- 26	- 29	- 32	- 36	-41
Resultant Total Counts/channel	96	98	168	245	241	139	26

5. The next step is to decide on the proper alpha peak width to use based on peak shape and height. To stay above the background due to the proton recoil tail and fission fragment tail, it is best to take a "slice" across the peak at 30% - 50% of the peak height. Then the same percentage must be used in taking peak widths across the fission fragment spectra. The counts ratio of the total (n, α) counts to fission fragment counts should be almost exactly the same regardless of pulse width as long as one stays sufficiently above background and sufficiently below the top of the peaks. Because there are few channels across the (n, α) peak, the idea is to use as many as possible to reduce statistical variation and the same number of channels is generally used from one run to the next. In Run #6, channels 13 - 18 were used for the (n, α) peak with a 39% peak height. Since the maximum number of counts in the

fission fragment channels was 449, only those fission fragment channels with counts above 39% or 175 were counted which were channels 32 - 51; 85 - 74. (See Figure 15.)

6. The source calibration was reasonably simple. Several calibration runs using the same ionization chamber were made outside the reactor. The naturally radioactive 2.236 mev peak of Sm^{147} and the two prominent uranium peaks, the 4.18 mev peak of U^{238} and the composite peak of 4.72 and 4.77 mev of U^{234}, are shown in the sample spectrum in Figure 16. To get the counts ratio of these two groups, i.e. A_t/A_{147} (see Chapter I, Part D of this thesis), one simply takes a peak width on the Sm^{147} peak that keeps counts in channels sufficiently above any background that might be present in the chamber and uses the same percentage of peak height for the uranium channels. The various calibration runs were used to find an average count ratio.

7. Finally the reaction cross section using Run #6 as an example can be calculated.

The effective cross section formula derived in Chapter I, Part D of this thesis is

$$\sigma = 186 \text{ millibarns } \frac{A_t}{A_{147}} \frac{A_{(n,\alpha)}}{A_f}.$$

For source #1 used in Run #6,

$$\frac{A_t}{A_{147}} = 1.33.$$

Therefore one finds.

$$\sigma = 247 \text{ m.b. } \frac{A_{(n,\alpha)}}{A_f}.$$

From Run #6 the resultant total of alpha counts in channels 13 - 18 after the proton recoil tail and the fission fragment tail have been subtracted out is $A(n,\alpha) = 987$ and $A_f = 10{,}041$ from channels 32 - 51 and 58 - 71.

Therefore the effective cross section is

$$\sigma(n, \alpha) = 247 \text{ m.b.} \frac{987}{10,041} = 24.3 \text{ m.b.}$$

Using the correction factor f = 1.83 from Section I-C of this thesis, the cross section for 2200 m/sec neutrons is:

$$\sigma(n, \alpha) = \frac{24.3}{1.83} \text{ m.b.} = 13.3 \text{ m.b.}$$

May 6 SM U Source 5watts,1 in. off bottom, 11 psi
050299 000000 000000 000001 000003 000002 023989 032930
004875 001268 001238 000731 000312 000231 000171 000139
000107 000133 000157 000169 000103 000050 000026 000037
000034 000035 000041 000040 000034 000038 000053 000040
000041 000043 000062 000069 000072 000072 00096 00115
000104 000110 000134 000164 000156 000181 000203 000186
000197 000216 000205 000202 000205 000198 000166 000158
000160 000193 000130 000127 000119 000116 000111 000108
000079 000104 00087 000096 000075 000101 000105 000105
000085 000109 000100 000106 000135 000114 00115 000136
000137 000137 000146 000129 000151 000147 000149 000132
000132 000112 000114 000095 000102 000101 000089 000079
000055 000052 000046 000057 000049 000043 000039 000038
000027 000029 000029 000028 000016 000023 000015 000016
000014 000010 000011 000008 000007 000003 000006 000005
00008 000002 000004 000000 000005 000000 000000 000002

Run #4

Same as above with 13 psi
092984 0000 000000 000012 000010 000013 057469 071135
011636 002764 002276 001349 000623 000480 000326 000293
000254 000260 000330 000301 000168 000068 000077 00075
000071 00072 000085 000086 000090 000103 000111 000136
000142 000155 000195 000188 000231 000270 000326 000349
000372 000434 000535 000502 000459 000520 000459 000453
000408 000414 000345 000327 000275 000255 000214 000220
000190 000204 000174 000155 000166 000179 000197 000164
000190 000200 000212 000200 000237 000232 000310 000270
000308 000331 000347 000299 000292 000308 000260 000282
000241 000223 000189 000170 000148 000148 000129 000114
000111 000093 000085 000060 000053 000038 000058 000049
000039 000036 000026 000025 000021 000018 000021 000012
000017 000008 000006 000011 000007 000009 000008 000000
000003 000001 000003 000000 000001 000002 000000 000000
000001 000000 000001 000000 000000 000000 000000 000000

Run #5

792984 Short RC, all the way, 13 psi
051965051965 000000 000000 000002 000003 00007 031255 043646
005791 002165 001421 000664 000423 000332 000231 000251
000304 000299 00184 000071 000074 000055 000057 000063
000072 00091 000088 000085 000108 000112 000120 000149
000189 000207 000217 000251 000332 000367 000380 000410
000414 000449 000402 000403 000321 000311 000277 000269
000247 000213 000226 000171 000160 000159 000168 000175
000160 000147 000173 000184 000204 000199 000220 000232
000260 000275 000320 000276 000257 000285 000258 000269
000213 000179 000181 000164 000162 000126 000092 000109
000089 000083 000071 000043 000064 000046 000039 000040
000023 000024 000029 000029 000027 000020 000015 000011
000012 000017 000014 000004 000006 000006 000005 000003
000005 000001 000001 000001 000000 000001 000000 000001
1 in. off bottom

Run #6

Figure 13. Sample Data Sheet (Source #1, Runs 4, 5 and 6).

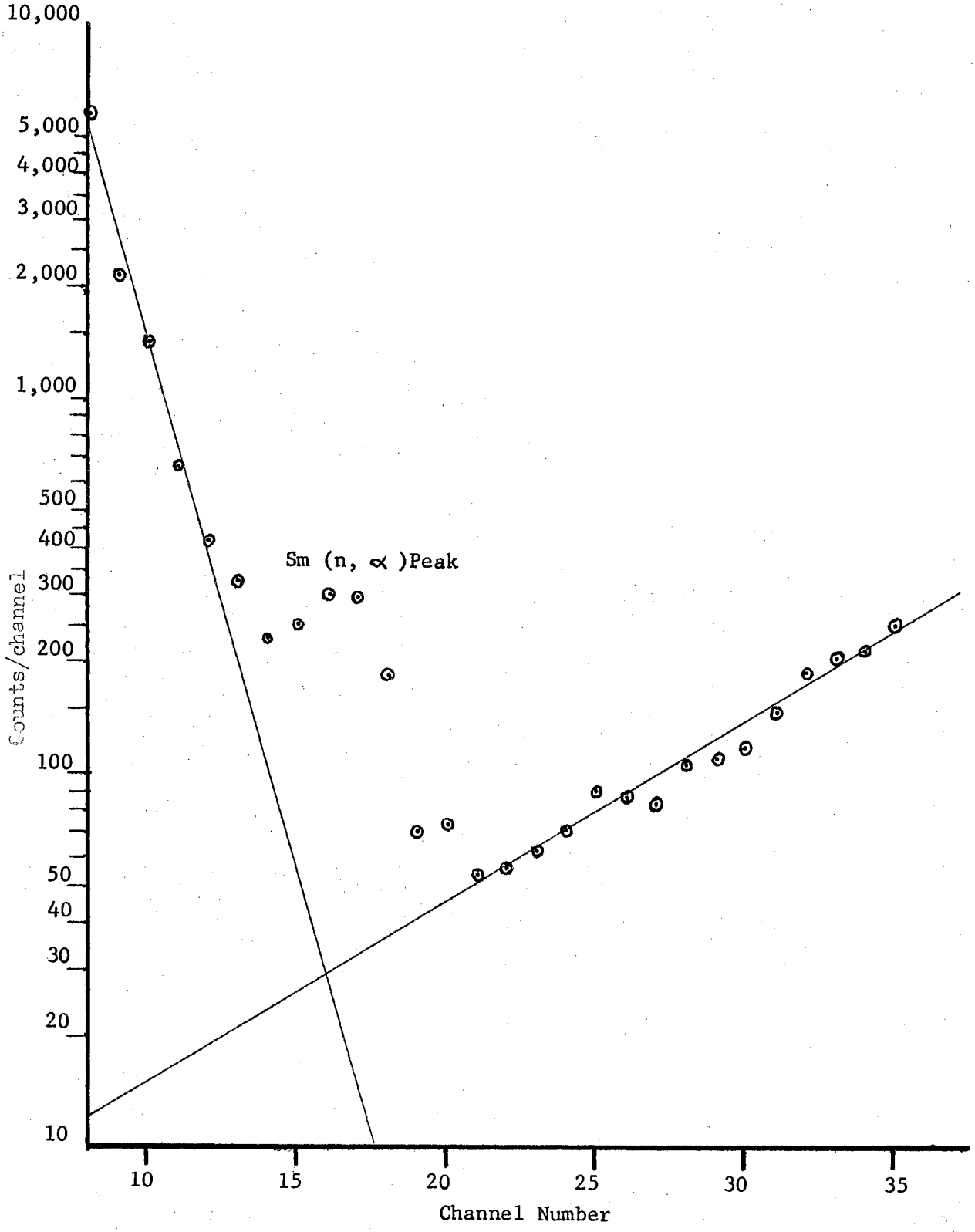

Figure 14. Sample Semilogarithmic Plot of Data (Source #1, Run #6).

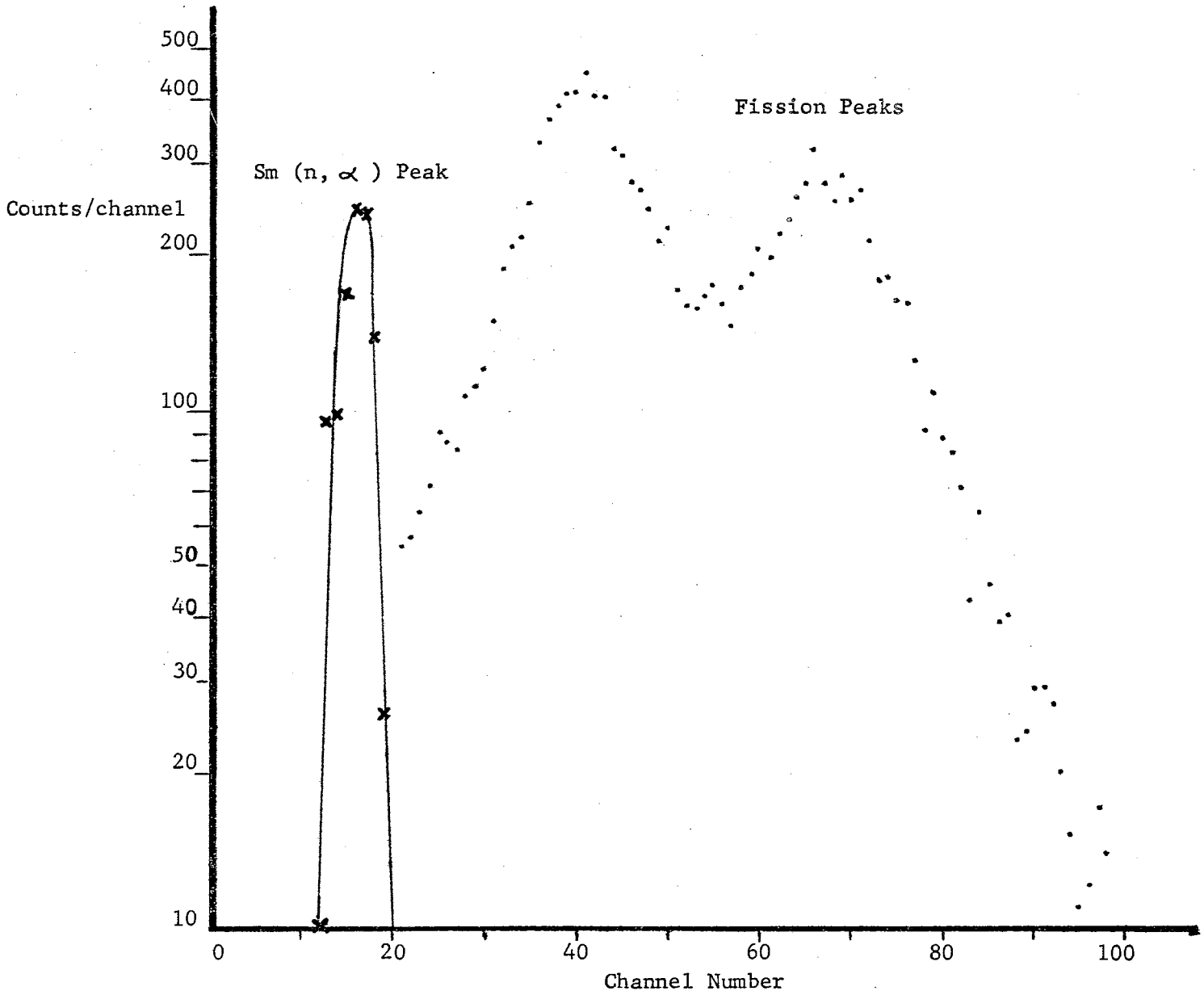

Figure 15. Resultant (n, α) Spectrum (Background Removed) and Fission Fragment Spectrum (Source #1, Run #6).

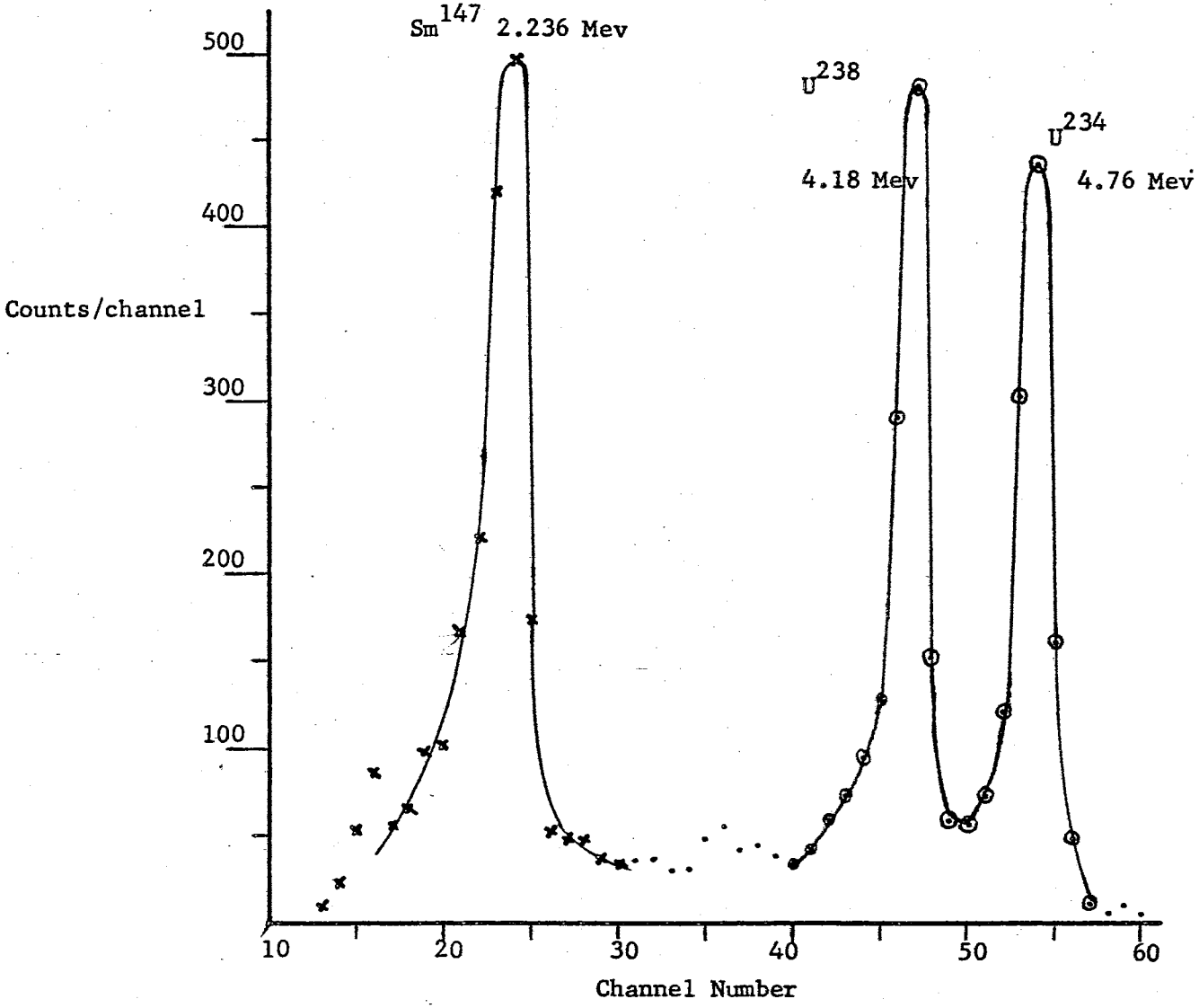

Figure 16. Sample Source Calibration Spectrum (Source #1, Run #2).

B. Summary of Results.

In Table III, the series of experimental runs made in the Oklahoma University Reactor is listed with the cross section value calculated from each. The average value was obtained for all runs and the root mean square deviation

$$D_{rms} = \sqrt{\sum_{i=1}^{n} \frac{\Delta_i^2}{n-1}}$$

was found for the deviation between runs.

TABLE III

CALCULATED EFFECTIVE CROSS SECTION VALUES

Source #1	Run No.	Cross Section (m.b.)
$A_t/A_{147} = 1.33$	1	19.3
	2	19.9
	3	24.7
	4	19.5
	5	18.2
	6	24.3
	7	24.4
	8	23.2
	9	19.5
	10	14.3
Average Value		20.6 m.b.
Source #2		
$A_t/A_{147} = .561$	1	18.7
	2	27.4
	3	23.9
Average Value		23.3 m.b.

Average cross section value for all runs:

$$\sigma(n, \alpha) = 21.3 \text{ m.b.}$$

Root mean square deviation for all runs:

$$D_{rms} = 3.9 \text{ m.b.}$$

The quoted value in this thesis for the effective cross-section measurement is:

$$\sigma(n, \alpha) = 21 \pm 4 \text{ m.b.}$$

The quoted value in this thesis for the cross section for 2200 m/sec neutrons using f = 1.83 is:

$$\sigma_o(n, \alpha) = 11.5 \pm 2.2 \text{ m.b.}$$

C. Problems Associated with Measurements and Suggested Means for Improvement.

The fundamental problem in using a gas ionization chamber in a reactor is the background pulses which result from the collisions of fast neutrons with the methane molecules in the (Argon 90%-Methane 10%) nuclear counter mixture causing proton recoil. This background depends on the fast to thermal neutron ratio of the reactor used. In the Oklahoma University reactor (Aerojet AGN 211) with an average thermal neutron temperature of 55^{0} C reactions below about 8 mev could not be observed using present equipment. It was thought that elimination of the methane might reduce the background. Therefore a 95% Argon - 5% CO_2 mixture was tried. The spectrum using this mixture in the ionization chamber lacked good energy resolution, and the background was only slightly reduced. It is possible that there was a contaminant in the mixture which was purchased for the experiment so there may still be a possibility that some combination of these two gases or some other gases might give a slightly improved resolution and lower background. However in order to observe reactions at 3.00 or 5.00 mev, using a reactor with a favorably low ratio of fast to thermal neutrons might be the best solution. Fortunately in the experiment described in this thesis, the energy of the reaction alpha was sufficiently above the background to be properly resolved.

The gas pressure used will affect the resolution of the spectra obtained from the ionization chamber positioned in the reactor. The optimum gas pressure was usually in the vicinity of 15 p.s.i. (above atmospheric pressure), but the best value had to be found experimentally.

The best irradiating position within the reactor also had to be found experimentally and seemed to vary slightly depending on reactor power level. In the Oklahoma University reactor, better resolution was usually obtained by not positioning the ionization chamber within the interior shielding of the reactor core which is an available position through one entry port. The optimum position in terms of fast to thermal neutron ratio seemed to be in the tube which went through the water and terminated just at the wall of the graphite jacket shielding the core, and the ionization chamber was usually set back about 4 inches from that end. This is a matter of reactor geometry.

This experiment did prove that a gas ionization chamber can be used in a thermal neutron flux inside a reactor for alpha spectrometry, and a cross-section measurement for the Sm^{149} (n, α) reaction was accomplished. The quoted value for effective cross section in this thesis is given in terms of the average value for all runs and the root mean square deviation of those runs. The range of experimental error for this experiment could not be easily estimated, but, considering some of the possible sources of error, this experimenter estimates that the range of error will overlap the cross section measurement made by the Israel AEC group (1) which was $\sigma = 42 \pm 10$ m.b. (neutron temperature not given). This means that the results of this thesis correlate with the results of the Israel AEC group and differ from a higher value published by the University of California research group (2) of $\sigma_{33^\circ C} = 233 \pm 29$ m.b. and $\sigma_o = 143 \pm 18$ m.b. The development of the type of equipment used in this experiment may make possible the observation of other (n, α) and (n, p) reactions such as those proposed by M. Mashat at Oklahoma State University (7), and enable one to verify or

improve measurements of such reactions which are known.

REFERENCES

1. E. Cheifetz, J. Gilat, A. I. Yavin, and S. G. Cohen, Physics Letters, Vol. 1, No. 7, 289-290 (1962).

2. R. D. MacFarlane and I. Almodovar, Phys. Rev., 127, 1665 (1962).

3. J. M. Blatt and V. F. Weisskopf, Theoretical Nuclear Physics (J. Wiley & Sons, 1952), p. 311.

4. Donald J. Hughes, Neutron Cross Sections (Pergammon Press, 1957).

5. V. B. Bhanot, W. H. Johnson, Jr., and A. O. Nier, Phys. Rev., 120, 241 (1960).

6. W. H. Johnson, Jr. and A. O. Nier, Phys. Rev., 105, 1015 (1957).

7. Mohammad Marouf Mashat, "The (n, α) Reaction Cross Section Induced by Thermal Neutrons", M.S. Report, Oklahoma State University, 1963.

8. N. J. Pattenden, "Proceedings of the Second United Nations International Conference on the Peaceful Uses of Atomic Energy, Geneva, 1958", (United Nations, Geneva 1958), Vol. 16.

9. Albert E. Wilson, Chief Reactor Operator, Oklahoma University, (Private communication).

10. Irving Kaplan, Nuclear Physics (Addison-Wesley, 1963), 2nd Ed., p. 214.

11. R. D. Evans, The Atomic Nucleus (McGraw-Hill, 1955), p. 484.

12. United States Atomic Energy Commission, Chart of The Nuclides (Published by General Electric Co., 1962), Revised Edition Dec. 1961.

13. E. Bleuber and G. F. Goldsmith, Experimental Nucleonics (Rinehart & Company, 1958), pp. 49-52.

14. E. Segre, Experimental Nuclear Physics (J. Wiley & Sons, 1953), Vol. 1.

15. Wayne L. Sievers, "The Half-lives of Bismuth-215 and Bismuth-211 and the Branching Ratio of Bismuth-211", M.S. Thesis, Oklahoma State University, 1963, Chap. II.

16. Jacob Millman, Vacuum Tubes and Semi Conductor Electronics (McGraw-Hill, 1958), pp. 80-81.

VITA

Charles Wain Friend

Candidate for the Degree of

Master of Science

Thesis: Sm^{149} (n, α) REACTION CROSS-SECTION MEASUREMENT USING A GAS IONIZATION CHAMBER

Major Field: Physics

Biographical:

Personal Data: Born in Stillwater, Oklahoma, August 17, 1937, the son of Earl H. and Mabel H. Friend.

Education: Graduated from Salem Senior High School, Salem. Oregon. Received Bachelor of Science degree from Oklahoma State University, Stillwater, Oklahoma, in May 1958; completed requirements for the Master of Science degree in May 1964.